Troglitazone Derivatives Induce Early Modifications of the Cytoskeleton and Inhibition of Migration in Breast Cancer Cells

Geoffroy Marine
UMR 7039: Centre de recherche en automatique de Nancy
Lemesle Marine
UMR 7039: Centre de recherche en automatique de Nancy
Kleinclauss Alexandra
UMR 7039: Centre de recherche en automatique de Nancy
Mazerbourg Sabine
UMR 7039: Centre de recherche en automatique de Nancy
Batista Levy
UMR 7039: Centre de recherche en automatique de Nancy
BarberiHeyob Muriel
UMR 7039: Centre de recherche en automatique de Nancy
Bastogne Thierry
UMR 7039: Centre de recherche en automatique de Nancy
Boireau Wilfrid
FEMTO-ST Département d'optique: Franche-Comte Electronique Mecanique Thermique et Optique Sciences et Technologies Departement d'optique
Alain Rouleau
FEMTO-ST Département d'optique: Franche-Comte Electronique Mecanique Thermique et Optique Sciences et Technologies Departement d'optique
Dupommier Dorian
CNRS: Centre National de la Recherche Scientifique
Boisbrun Michel
Universite de Lorraine
Comoy Corinne
Université de Lorraine: Universite de Lorraine
Flament Stéphane
UMR 7039: Centre de recherche en automatique de Nancy
Isabelle Grillier-Vuissoz (isabelle.grillier-Vuissoz@univ-lorraine.fr)
Universite de Lorraine, CRAN UMR 7039 https://orcid.org/0000-0002-9820-3804
Kuntz Sandra

UMR 7039: Centre de recherche en automatique de Nancy

Research Article

Keywords: Breast cancer, Troglitazone derivatives, Apoptosis, Cytoskeleton, tubulin, Cell migration.

Posted Date: October 18th, 2021

DOI: https://doi.org/10.21203/rs.3.rs-911353/v1

Troglitazone derivatives induce early modifications of the cytoskeleton and inhibition of migration in breast cancer cells

Geoffroy Marine[1], Lemesle Marine[1], Kleinclauss Alexandra[1], Mazerbourg Sabine [1], Batista Levy[1], Barberi-Heyob Muriel[1], Bastogne Thierry[1], Boireau Wilfrid[3], Rouleau Alain[3], Dupommier Dorian[2], Boisbrun Michel[2], Comoy Corinne[2], Flament Stéphane[1], Grillier-Vuissoz Isabelle[1*], Kuntz Sandra[1*]

I. Grillier-Vuissoz and S. Kuntz contributed equally to the co-supervising of this study

Corresponding author:
I Grillier-Vuissoz:
Tel: +33 (0)3 72 74 51 84
E-mail: isabelle.grillier-vuissoz@univ-lorraine.fr

[1] Université de Lorraine, CNRS, CRAN, F-54000, Nancy, France
[2] Université de Lorraine, CNRS, L2CM, F-54000, Nancy, France
[3] FEMTO-ST Institute, CNRS, Université de Bourgogne Franche-Comté, F-25030 Besançon, France

Abstract

Background: The 5-years survival rate of breast cancer patients is around 90%. Unfortunately, some types of tumors, especially the triple negative breast cancer (TNBC), present chemo-resistance and have a higher relapse 5 years post-treatment due to metastasis. These challenges highlight the need for the development of new drugs for these tumors. In this context, we developed new troglitazone derivatives as support for such potential new treatment.

Methods: The kinetic of early cellular events was investigated after Δ2-TGZ and AB186 treatment by real-time cell analysis system (RTCA) in MCF-7 and MDA-MB-231 breast cancer cells, followed by cell morphology analysis by immuno-localization. Then, we characterized the action of both compounds on the cell migration by wound healing and transwell assays in TNBC MDA-MB-231 and Hs578T cell lines. Finally, we performed surface plasmon resonance (SPR) analysis and pull-down assay using biotinylated AB186 to identify cytoplasmic targets.

Results: Δ2-TGZ and AB186 induced a rapid modification of impedance-based signals and morphology in MCF-7 and MDA-MB-231 breast cancer cell lines. This process was associated with an inhibition of cell migration in MDA-MB-231 and Hs578T cell lines. Subsequently, 6 cytoskeleton components have been identified as potential targets of AB186 in MDA-MB-231 cytoplasmic fraction. We further validated α-tubulin as one of the direct targets of AB186.

Conclusion: New troglitazone derivatives, Δ2-TGZ and AB186, induced early cell morphological changes and showed anti-migratory effects on TNBC cells suggesting that these drugs could be proposed as novel candidates to treat TNBC patients.

Keywords: Breast cancer, Troglitazone derivatives, Apoptosis, Cytoskeleton, tubulin, Cell migration.

Introduction

Breast cancer is one of the leading causes of cancer-related death among females worldwide [1]. Breast tumors are classified by the presence of three molecular markers: estrogen receptor (ER), progesterone receptor (PR) and human epidermal growth factor receptor 2 (HER2), that allow targeted therapy beside chemotherapy [2]. Nevertheless, the effects of therapeutic agents are limited by *de novo* or acquired resistance and they often cannot avoid the metastatic spread [3, 4]. Triple negative breast cancer (TNBC) subtype (ERα-, PR-, HER2-) presents the worst prognostic due to its highly invasive nature and relatively low response to therapeutics [5]. Therefore, there is an urgent need to develop alternative therapeutics.

Troglitazone (TGZ) is a synthetic compound of the thiazolidinediones (TZDs) family like rosiglitazone (RGZ) and pioglitazone (PGZ), used as antidiabetic agents. TZDs also display anti-tumoral activity not only *in vitro* but also *in vivo* [6, 7]. Despite promising *in vitro* data and pre-clinical studies highlighting the strong potential of TZDs in breast cancer treatment, clinical trials did not display clear beneficial effects. Their anticancer properties were recently renewed by a phase II trial on chronic myeloid leukemia. This study provided evidence that in combination with imatinib, PGZ improved the erosion of the cancer stem cells pool [8, 9]. Similarly, a clinical study indicated that efatutazone associated with paclitaxel could be effective in anaplastic thyroid carcinoma [10]. More recently, Ronen *et al.* showed that RGZ in combination with MEK inhibitors enhanced epithelial differentiation and adipogenesis of breast cancer cells both *in vitro* and *in vivo* [11]. Unfortunately, the majority of TZDs were withdrawn from the market because of their side effects, especially severe hepatic toxicity for troglitazone [12]. In this context, our team developed new TGZ derivatives that are more potent and less toxic. We synthetized the already known Δ2-troglitazone (Δ2-TGZ) and also the original molecule AB186 (Figure 1) [13–15]. TGZ is a PPARγ agonist, nevertheless many of its anticancer activities are PPARγ independent [6]. Here, both Δ2-TGZ and AB186 are devoid of PPAR γ agonist activity. Indeed, we and other established that the introduction of a double bond adjoining the terminal thiazolidine-2,4-dione ring of TGZ abrogated the PPARγ agonist activity [16–19]. The loss of PPARγ activity was explained by the structural rigidity induced by this double bond surrounding the TZD ring [19]. Furthermore, AB186 is deoxygenated on the chromane moiety and holds at this position an aminoalkyl chain, both inducing higher efficiency to inhibit cell proliferation of breast cancer cells MCF-7 and MDA-MB-231 [14].

Previously, we have demonstrated that compared to TGZ, Δ2-TGZ and AB186 exhibit a lower toxicity towards human non-malignant hepatocytes in primary culture and an improved anti-proliferative activity on breast cancer cell lines [13, 14]. We showed that Δ2-TGZ induced apoptosis in luminal cells MCF-7 and in MDA-MB-231 and Hs578T TNBC cells [20, 21]. In the present study, we aimed to better understand the mechanism of action of Δ2-TGZ and AB186. Starting at 24 h, we showed a stronger pro-apoptotic effect of AB186 compared to Δ2-TGZ in breast cancer cells and interestingly not in the non-tumoral MCF10A cells. Then, we analyzed the dynamic

response to Δ2-TGZ and AB186 using a real-time cell analysis on MCF-7 and MDA-MB-231 cells. We observed a rapid modification of impedance and morphological cellular changes. These modifications were rapidly followed by cell migration inhibition in MDA-MB-231 and Hs578T TNBC cells. Both events suggested interactions with cytoskeleton proteins. In order to identify the targets of AB186, we performed Surface Plasmon Resonance (SPR) analysis that comforted this hypothesis. We identified 6 targets from the cytoskeleton: γ-actin, β-tubulin, filamin-A, α-tubulin, moesin, talin. Pull-down assays in MDA-MB-231 and Hs578T and *in vitro* tubulin polymerization assays highlighted the binding of AB186 to α-tubulin.

Materials and methods

Materials

The synthesis of Δ2-TGZ and AB186 were performed as previously described [13, 14]. In stock solutions, both compounds were dissolved at 50 mM in DMSO. The synthesis of biotinylated and rhodamin linked AB186 compounds are described in supplementary data (**supplementary data.1**). The human breast cancer and the non-tumorigenic human breast epithelial cell lines were purchased from the American Type Culture Collection. Dulbecco's modified Eagle medium (DMEM), DMEM/F12, RPMI Medium 1640 (RPMI), Trypsin-EDTA and PBS were purchased from Life Technologies. Ethanol (EtOH), dimethylsulfoxide (DMSO), fetal calf serum (FCS), horse serum, human epidermal growth factor (hEGF), L-glutamine, bovine insulin, hydrocortisone and cholera toxin were purchased from Sigma-Aldrich.

Methods

Cell culture and treatment

MCF-7 and MDA-MB-231 cell lines were cultured at 37°C under 5% CO_2 in phenol red DMEM and RPMI respectively, supplemented with 10% FCS and 2 mM L-glutamine. Hs578T cells were grown in DMEM containing phenol red supplemented with 10% FCS, 2 mM L-glutamine and 10 µg/mL bovine insulin. MCF-10A cells were grown in DMEM/F12 supplemented with 5% horse serum, 2 mM L-glutamine, 100 U/mL penicillin, 100 µg/mL streptomycin, 10 µg/mL bovine insulin, 0.5 µg/mL hydrocortisone, 100 ng/mL cholera toxin and 20 ng/mL hEGF. Cells were treated with 0.01% DMSO (vehicle) or various concentrations of Δ2-TGZ and AB186 in 1% FCS containing medium.

Flow cytometry

MDA-MB-231 (4.10^5 cells/well) and MCF-10A ($1.5.10^5$ cells/well) cells were seeded in 6-well plates and treated with DMSO (vehicle), 20 µM of Δ2-TGZ or 4 µM of AB186 for 24 h or 48 h. Then, flow cytometry analyses were performed as described previously [21].

Real-time impedance-based cell analysis

MCF-7 (8.10^3 cells/well) and MDA-MB-231 (4.10^3 cells/well) cells were seeded into 96-wells microelectronic standard E-plate and grown during 29 h before exposure to DMSO, Δ2-TGZ or AB186. MCF-7 and MDA-MB-231 cells attachment, proliferation and size variations were monitored in real-time and measured as impedance

using the xCELLigence system (Real Time Cell Analyzer Single Plate (RTCA SPH) system) (Roche Applied Science, Mannheim, Germany) [22]. Cell index (CI) is an arbitrary unit representing the result of the impedance induced by adherent cells to the electron flow. CI was calculated as follows: CI= (impedance at time point n - impedance in the absence of cells)/nominal impedance value. Background impedance of the E-Plate was first determined before seeding the cells by the addition of 50 µL culture medium to each well and subtracted automatically by the RTCA software following the equation: CI = (Zi-Z0)/15 with Zi as the impedance at any given time point and Z0 as the background signal. Impedance measurement were performed every 15 min intervals.

Immunofluorescence

MCF-7 (4.10^4 cells/well) and MDA-MB-231 (8.10^4 cells/well) were seeded in 24-well plates on coverslips and treated with Δ2-TGZ or AB186 for different times. Then, immunofluorescence experiments were performed as described previously [21]. Polymeric F-actin filaments were labelled with Phalloïdin conjugated to Alexa Fluor 488 (A12379, Thermofisher Scientific) diluted to 1:30. Microtubules and intermediate filaments were labelled with α-tubulin (GTX102079, GeneTex) and vimentin (MAB1633, Chemicon) antibodies, respectively, diluted to 1:250. MDA-MB-231 (3.10^5 cells/well) were also seeded in 12-well plates on coverslips and exposed to 3 µM of rhodamine-labelled AB186 (ABRhod) or unlabeled compound (Control) during 1 and 6 h. Then, cells were fixed with 4% of paraformaldehyde and nuclei were labelled with Hoechst. Fluorescence labeling was observed under an Eclipse 80i microscope and images were collected using NIS-Elements Basic Research software (Nikon, Champigny sur Marne, France).

Wound healing assay

MDA-MB-231 (6.10^5 cells/well) and Hs578T (2.10^5 cells/well) were seeded in 6-well plates for 24 h until 90 % of confluence. A scratch was made with a 200 µL pipette tip through the cell monolayer and cells were treated with Δ2-TGZ or AB186 for 0, 3, 6 or 12 h. Wound closure was observed as previously described [23].

Migration assay

MDA-MB-231 (13750 cells/well) and Hs578T (13750 cells/well) were seeded in the upper chamber of Transwell membranes (6.5 mm Transwell® 8.0 µm pore Polyester Membrane Insert, #3464, Corning) and treated with Δ2-TGZ or AB186 in medium supplemented with 1% FCS. The upper chamber of insert containing cells was placed into the lower chamber supplemented with 10% FCS as chemoattractant. After 9 h of treatment, the migrating cells were analyzed as described previously [23].

SPR binding analysis

Cytoplasmic proteins of MDA-MB-231 cells were extracted using the ProteoExtract® Subcellular Proteome Extraction Kit following manufacturer instructions (Merk Millipore). The cytoplasmic fraction was filtrated through a 0.2 µm microspin Costar at 10 000 g for 7 min at 4°C. Proteins were diluted to 5 µg/mL with PBS 1X before Surface Plasmon Resonance analysis on AB186 hybridized chips (**supplementary data.2**).

Pull down assay

Pull-down assay was performed with Dynabeads M-280 Streptavidin (Life Technologies) according to the manufacturer's protocol. Briefly, 50 mM of biotinylated AB186 were fixed to the microbeads during 20 min at room temperature under agitation. Then, the microbeads were washed three times with 0.1 % Triton X-100 in PBS buffer and 400 µg of proteins were added during 40 min at 4°C under agitation. For the control, proteins were incubated with the microbeads without biotinylated AB186. After washing, proteins were re-suspended in lysis buffer while the beads were removed with a magnet and the protein were subjected to western blot as described previously [21]. The antibodies raised against β-actin (SC-1615, Santa Cruz) and α-tubulin (GTX102079, GeneTex) were diluted at 1:5000 and 1:4000 respectively.

Tubulin polymerization assay

The effect of AB186 on tubulin assembly was measured using the In Vitro Tubulin Polymerization Assay Kit according to the manufacturer's instructions (Millipore). Briefly, polymerization reactions occur in 70 µL final volume of 1x polymerization buffer (PB)-GTP (1mM final), of which 60 µL is the 60 µM tubulin and 10 µL is the test substance AB186 (5 µM) or paclitaxel (PTX) (10 µM) or DMSO (control). Tubulin assembly was measured by spectrophotometry every 30 seconds at 350 nm during 90 minutes at 37 °C.

Statistical analysis

The results of each experiment were expressed as mean ± standard error of the mean (SEM) of three to six different experiments. Statistical differences were determined using Student's *t* test or ANOVA test with Bonferroni post-hoc. Differences in which P was less than 0.05 were statistically significant (SPSS v11.0 Computer Software).

Results

1. AB186 is a more potent inducer of apoptosis compared to Δ2-TGZ in MDA-MB-231 breast cancer cells and is ineffective in the non-malignant MCF10A

AB186 is a new TGZ derivative which possesses, in addition to the double bond (1) adjoining the thiazolidine-2,4-dione ring as in Δ2-TGZ, a deoxygenation of the chromane heterocycle (2) and a hydrophobic aminoalkyl moiety (3) (**Figure 1**). In a previous study, we demonstrated that Δ2-TGZ induced apoptosis after 24 h of treatment in MDA-MB-231 breast cancer cells but not in non-tumorigenic mammary cells MCF-10A [21]. We exposed these cells to 4 µM of AB186, a dose that was just above the cell viability IC_{50} that we previously measured in MDA-MB-231 [14]. AB186 also led significantly to the apoptosis of MDA-MB-231 breast cancer cells but not of MCF-10A cells (**Figure 2**). After 24 h of exposure, 4 µM of AB186 induced 44 % of apoptotic cells while 20 µM of Δ2-TGZ was required to obtain 32 % of apoptotic cells. Likewise, after 48 h of treatment, Δ2-TGZ and AB186 induced 51 % and 55 % of apoptotic cells respectively. Thus, AB186 (4 µM) induced a higher or similar apoptosis rate at a 5-fold lower dose compared to Δ2-TGZ (20 µM) in these breast cancer cells.

2. Variations of impedance occur early after Δ2-TGZ and AB186 treatment in MCF-7 and MDA-MB-231 breast cancer cells

In order to investigate the kinetics of events leading to the anticancer effect of Δ2-TGZ and AB186, we performed a real-time cell analysis (RTCA) allowing the measurement of impedance-based signals. MCF-7 and MDA-MB-231 cells were exposed to Δ2-TGZ (25 µM and 20 µM respectively) or AB186 (5 µM and 4 µM respectively). In both control cells, the Cell Index value increased progressively until the end of the experiment to reach 2.4 and 1.9 in MCF-7 and MDA-MB-231 respectively. In both cell lines, CI kinetics were modified after Δ2-TGZ and AB186 exposure compared to the control cells and we noted a rapid and transient increase of CI in response to both compounds. Finally, after 24 h, the CI decreased to reach a value equal or below those measured at the beginning of treatment (**Figure 3**).

In order to better correlate the impedance modifications to a biological effect, we determined the time of maximal difference of CI between control and treated cells (**Table 1**). In MCF-7 cells, this key time point was observed at 1 h 55±8min and 4 h±75min in response to Δ2-TGZ and AB186 respectively (**Figure 3A, Table 1**). In MDA-MB-231 cells, the CI reached a maximal difference at 1 h 50±5min and 3 h 55±13min after Δ2-TGZ and AB186 exposure respectively (**Figure 3B, Table 1**). These data suggest early modifications induced by Δ2-TGZ and AB186 before apoptosis.

3. Δ2-TGZ and AB186 induce early morphological changes in MCF-7 and MDA-MB-231 breast cancer cells

On the basis of the early maximal difference of CI obtained by impedance analysis, we hypothesized that morphological changes could be involved in this observation. After 2 h 30, 4 h 30, 8 h 30 or 10 h 30 of TGZ derivatives treatment, we analyzed by immunofluorescence the morphology of MCF-7 and MDA-MB-231 cells using three cytoskeletal constituents: actin, α-tubulin and vimentin. The control MCF-7 cells displayed a cobblestone-like phenotype with strong cell-cell adhesion (**Figure 4A**). In response to Δ2-TGZ and AB186, MCF-7 cell morphology was altered by changes in cell shape and size (**Figure 4B and 4C**). We observed some elongated cells around 4 h 30 of exposure to Δ2-TGZ and AB186 and some shrunken cells with condensed chromatin after 8 h 30 of treatment. At 10 h 30 of treatment, almost all cells were shrunken. Control MDA-MB-231 cells displayed a fibroblast-like morphology with a pronounced cellular scattering (**Figure 5A**). In response to Δ2-TGZ and AB186, MDA-MB-231 cell morphology was also altered with elongated cells harboring an unorganized actin network from 2 h 30 of treatment (**Figure 5B and 5C**). As observed in MCF-7 cells, both treatments led to shrunken cells from 8 h 30 exposure in MDA-MB-231 cells.

4. Δ2-TGZ and AB186 inhibit migration properties of two highly metastatic TNBC cell lines: MDA-MB-231 and Hs578T

The modifications of cell shape and the disruption of cytoskeleton induced by Δ2-TGZ and AB186 suggested that these compounds could modify the migration potency of the cells. Indeed, it is well described that cytoskeleton modifications can influence cell migration properties [24]. To determine whether Δ2-TGZ and AB186 could affect cell migration, we performed migration assays on MDA-MB-231 and Hs578T, two TNBC cell lines with highly metastatic properties. First, both cells were exposed to TGZ derivatives and wound healing assay was performed after 3, 6 and 12 h of treatment. We observed a significant wound healing inhibition at 6 h of exposure to Δ2-TGZ and AB186 in MDA-MB-231 cells. In Hs578T cells, we also observed an inhibition of wound healing that was significant at 6 h and 12 h of Δ2-TGZ and AB186 treatment respectively (**Figure 6A**). Then, we confirmed these

results using the transwell assay after 9 h of exposure to the TGZ derivatives. In MDA-MB-231 cells, the number of migrated cells exhibited a significant decrease of 27.16% and 34.70% after Δ2-TGZ and AB186 treatment, respectively, compared to control cells. In the same way, Δ2-TGZ and AB186 reduced significantly the migration by 41.11% and 49.33% respectively in Hs578T cells compared to control cells (**Figure 6B**).

5. AB186 acts through the binding to the cytoskeleton component: α-tubulin

Early morphological changes mediated by TGZ derivatives could be explained by the interaction between the drug and the cytoskeleton. In order to determine the localization of AB186 in the cell, we exposed MDA-MB-231 cells to rhodamine-labelled AB186 (ABRhod, see supplementary material) for 1 or 6 h. The signal was diffuse after 1 h and concentrated in the cytoplasm after 6 h (**Figure 7**). To identify direct cytoplasmic targets of AB186, a SPR binding analysis was performed using MDA-MB-231 cytoplasmic extracts and AB186 immobilized on sensor chips [25]. On-Chip mass spectrometry analysis revealed that AB186 could bind to 94 proteins including 6 cytoskeletal proteins, belonging to the similar GO pathways "structural molecule activity" (GO.0005198) and "structural constituent of cytoskeleton" (GO.0005200): γ-actin, β-tubulin, filamin-A, α-tubulin, moesin and talin (**Table 2**). By pull-down assay, we validated that biotinylated AB186 (ABBiot, see supplementary material) binds to α-tubulin in MDA-MB-231 and Hs578T cells while the interaction between AB186 and β-actin was observed only in MDA-MB-231 cells (**Figure 8A**). No clear interaction was confirmed with moesin and talin. In addition, AB186 promote tubulin polymerization into microtubules *in vitro*. Indeed, tubulin polymerization started earlier compared to the control condition (**Figure 8B**). AB186 displayed a different profile compared to paclitaxel, well known to promote microtubule assembly and affect microtubule dynamics. In the presence of AB186, the accumulation of polymerized tubulin started later than in the presence of paclitaxel. The morphology of microtubules was then examined in breast cancer cells by immunofluorescence microscopy (**Figure 8B**). At room temperature (RT), AB186 induced a dose-dependent enlargement of tubulin network, with elongated microtubules. Microtubules were more condensed and reorganized into thick ring-like bundles near the nucleus after paclitaxel treatment. Cold treatment was performed to study the stability of microtubules. As expected, in control cells, the microtubule network was altered by cold treatment. In presence of paclitaxel, no network remodeling was observed between RT and 4°C conditions. Interestingly, AB186 treatment induced a dose dependent stabilization of the network compared to control cells (**Figure 8C**).

Discussion

The chemo-resistance of TNBC tumors highlights the urgent need to develop new drugs in order to stretch the range of chemotherapy drugs to fight the acquired resistances. Here, we studied two TGZ derivatives, Δ2-TGZ and AB186, that we have previously shown to inhibit cell growth and to induce breast cancer cell death [14, 20]. Interestingly, AB186 is a more potent inhibitor of TNBC cell proliferation than efatutazone, a TZD used in combination with chemotherapy drug to treat cancer [14, 26]. Our aim was to better understand the mechanism of action of these two derivatives.

In order to investigate the kinetic of events leading to anti-cancerous effect of Δ2-TGZ and AB186, we measured cell impedance in real time. The profiles obtained from RTCA suggested a rapid modification of the cell morphology occurring between 2 and 4 h of treatment with these compounds in both MCF-7 and MDA-MB-231

cells. We then showed an inhibition of MDA-MB-231 and Hs578T cell migration as soon as 9 h of treatment by Δ2-TGZ or AB186. This result was consistent with the fact that TZDs have been reported to inhibit cancer cell motility *in vitro* and *in vivo* [27]. Several studies have shown that the inhibition of cell migration by TGZ was associated with a modification of cell morphology [28–30]. PK-1 (pancreas), ES-2 (ovary) and MDA-MB-231 (breast) cancer cells were smaller and their shape was modified to a spindle-shaped morphology. In PK-1 cells, the morphological changes induced by TGZ required a remodeling of actin network cells where TGZ inhibited lamellipodia formation and actin polymerization [28, 29]. Likewise, in ES-2 cells, TGZ reduced the number of focal adhesions related to actin stress fibers decrease [30]. Moreover, TGZ reduced cell adhesion and spreading of MDA-MB-231 after 1 h of treatment on fibronectin coated-plates [29]. In our study, we also observed changes in cell shape and size. At early time, cells stretched and formed cytoplasmic extensions, followed by a round shape after 10 h 30 of treatment suggesting cell death. These changes were associated with reorganization of tubulin and actin networks.

Using proteomic analyses, we identified 6 potential cytoskeleton targets of AB186: γ-actin, β-tubulin, filamin-A, α-tubulin, moesin and talin. Pull-down assay performed on MDA-MB-231 and Hs578T confirmed the binding of AB186 to α-tubulin. *In vitro* polymerization assay suggested that AB186 stimulated tubulin polymerization into microtubules. Immunofluorescence analysis showed a rapid enlargement and elongation of tubulin network, in agreement with the early maximal difference of CI measured by impedance analysis. This enlargement could result in stronger adhesion properties as previously observed [31]. It remains unclear at present how AB186 exerts its effect on microtubule assembly and stability. It could act as a tubulin stabilizer by a different process than paclitaxel. One may suggest that it could work similarly to Mdp3, a microtubule-binding protein that regulates microtubule assembly and stability [32]. Our results corroborate a previous study suggesting that TZDs could act as cytoskeleton binding molecules [33]. The exact consequences of AB186 interaction with α-tubulin need to be investigated. Interestingly, new microtubules inhibitors have been developed recently in order to treat TNBC [34, 35].

In conclusion, we determined that AB186 was a potent pro-apoptotic agent in breast cancer cells. We further characterized early modifications of cell morphology followed by the inhibition of cell migration after Δ2-TGZ and AB186 treatment. We identified for the first-time cytoskeleton targets for AB186 that could explain the early morphological changes and migration inhibition. Overall, these data suggest that AB186 could be a promising TZD molecule for TNBC treatment regarding its anti-migratory and pro-apoptotic properties.

Acknowledgments and Funding information This work was supported by grants of the “Université de Lorraine”, the “Conseil Régional du Grand Est”, “Cancéropôle Est” and the “Ligue Contre le Cancer”.
Marine Geoffroy, Marine Lemesle and Dorian Dupommier were recipients of a PhD grant of the « Ministère de l’Enseignement Supérieur, de la Recherche et de l’Innovation ».
We thank Elodie Cortelazzo-Polisini and Arnaud Risler from L2CM laboratory for the realization of the *in vitro* tubulin polymerization assay.

Compliance with ethical standards

Disclosures and declarations: The authors declare that they have no conflict of interest.

Table 1. Maximal difference of cell index between control condition and treated condition, Δ2-TGZ/Control and AB186/Control, was determined for three independent experiments. The mean of maximal difference of CI for each treatment was determined in MCF-7 and MDA-MB-231 cells.

Table 2. Cystoskeleton proteins identified by MS analysis using Proteome Discoverer software. Corresponding peptides were obtained after biochemical treatments of the captured cytoplasmic proteins from MDA-MB-231 breast cancer cells on AB186-hybridized SPR chip. # Peptides: number of different peptides corresponding to a unique protein. Mascot Score: statistical score based on the probability that the peptides from the sample match those in the selected protein database.

Fig 1. Structure of TGZ, Δ2-TGZ and AB186 compounds. Δ2-TGZ and AB186 are derived from the original TGZ and both of them possess a double bond (1) adjoining the terminal thiazolidine-2,4-dione ring. AB186 also presents a deoxygenation of the chromane heterocycle (2) and a hydrophobic moiety (3).

Fig 2. AB186 induces apoptosis in MDA-MB-231 TNBC cells. After treatment for 24 and 48 h with DMSO (Ctrl), 20 µM of Δ2-TGZ or 4 µM of AB186, MDA-MB-231 and MCF-10A cells were co-stained with FITC-Annexin V/PI and analyzed by FACS. The percentage of total apoptotic cells corresponds to Annexin V positive cells and Annexin V/PI positive cells (dot plot of MDA-MB-231 cells exposed to 48 h of treatment). The values represent the means ± SEM of 3 to 6 different experiments. ANOVA test with Bonferroni post-hoc was used to determine significance difference from control cells, were $*p<0.05$ and $***p<0.001$.

Fig 3. Kinetics of real-time impedance changes in response to TGZ derivatives in MDA-MB-231 and MCF-7 cells. (A) MCF-7 and (B) MDA-MB-231 cells were grown during 29 h and then were exposed (treatment addition) to Δ2-TGZ (25 µM and 20 µM respectively) or AB186 (5 µM and 4 µM respectively). Control cells were treated with DMSO. Cell index was monitored during 24 h after treatment addition. Reported data are the means of three independent experiments.

Fig 4. TGZ derivatives alter MCF-7 morphology. MCF-7 cells were treated with DMSO as control (A), 25 µM of Δ2-TGZ (B) or 5 µM of AB186 (C) during 2 h 30, 4 h 30, 8 h 30 and 10 h 30. Then, cells were subjected to immunofluorescence analysis and stained with antibodies against vimentin, α-tubulin and actin. Cell nuclei were labelled with Hoechst dye. Bright field pictures of control and treated cells are also shown after 8h30. Δ2-TGZ and AB186 led to disruption of cell-cell contact compared to untreated cells. Elongated cells (white arrows) and some shrunken cells (yellow arrows) were observed. Bar represent 50 µm.

Fig 5. TGZ derivatives alter MDA-MB-231 morphology. MDA-MB-231 cells were treated with DMSO as control (A), 20 µM of Δ2-TGZ (B) or 4 µM of AB186 (C) during 2 h 30, 4 h 30, 8 h 30 and 10 h 30. Then, cells were subjected to immunofluorescence analysis and stained with antibodies raised against vimentin, α-tubulin and actin. Cell nuclei were labelled with Hoechst dye. Bright field pictures of control and treated cells are also shown after 8h30. Elongated cells (white arrows) and some shrunken cells (yellow arrows) were observed. Bar represent 50 µm.

Fig 6. TGZ derivatives alter migration properties of MDA-MB-231 and Hs578T cells. MDA-MB-231 and Hs578T cells were exposed to DMSO as control, or 20 µM of Δ2-TGZ or 4 µM of AB186 and subjected to wound healing (A) or transwell migration (B) assays. (A) Cell free area was measured after 3 h, 6 h and 12 h of TGZ derivatives exposure. Each wound healing corresponds to the mean of three different areas. (B) Cells were seeded in the upper chamber of Transwell membranes and treated with Δ2-TGZ or AB186 for 9 h. Graphs represent the average of migrated cells on the lower chamber. Reported data are the means of three or six experiments. Analysis of variance (ANOVA) was used to determine significant difference of migration from control cells, where $*p<0.05$, $**p<0.01$ and $***p<0.001$.

Fig 7. Rhodamin labelled AB186 localizes in the cytoplasm of MDA-MB-231 cells. MDA-MB-231 cells were exposed to 3 µM of Rhodamin labelled AB186 during 1 or 6 h. Control cells were exposed to the unlabeled compound. Cells were fixed with paraformaldehyde and cell nuclei were labelled with Hoechst dye. Bar represents 50 µm.

Fig 8. AB186 directly targets the microtubule cytoskeleton. (A) MDA-MB-231 and Hs578T cells lysate were incubated with the microbeads and biotinylated AB186 (ABBiot) for 40 minutes or in absence of AB186 (Ctrl). Precipitated proteins were then subjected to western blot analysis. Western blot analysis was performed using anti-α-tubulin and anti-β-actin antibodies. Input corresponds to the total lysate before pull-down assay. (B) *In vitro* tubulin polymerization assay was performed. Bovine tubulin was exposed to DMSO (Ctrl), 5 µM of AB186 or 10 µM paclitaxel. The tubulin polymerization rate was monitored during 90 min at 37°C and measured by absorbance at 350 nm. (C) MDA-MB-231 cells were treated with DMSO (Ctrl), AB186 (5, 10 or 20 µM) or paclitaxel (PTX) (5 µM) during 15 min at room temperature (RT) or 4°C. Then, cells were subjected to immunofluorescence analysis after staining with antibodies raised against α-tubulin. Cell nuclei were labelled with Hoechst dye. Representative high-resolution image focusing on one single cell in each group present a 6X magnification. Bar represent 10 µm.

Supplementary data 1. Synthesis of tagged derivatives of AB186.

Supplementary data 2. SPR binding analysis.

References

1. Bray F, Ferlay J, Soerjomataram I, et al (2018) Global cancer statistics 2018: GLOBOCAN estimates of incidence and mortality worldwide for 36 cancers in 185 countries. CA Cancer J Clin 68:394–424. https://doi.org/10.3322/caac.21492

2. Parise CA, Caggiano V (2014) Breast Cancer Survival Defined by the ER/PR/HER2 Subtypes and a Surrogate Classification according to Tumor Grade and Immunohistochemical Biomarkers. J Cancer Epidemiol 2014:469251. https://doi.org/10.1155/2014/469251

3. Early Breast Cancer Trialists' Collaborative Group (EBCTCG) (2005) Effects of chemotherapy and hormonal therapy for early breast cancer on recurrence and 15-year survival: an overview of the randomised trials. Lancet Lond Engl 365:1687–1717. https://doi.org/10.1016/S0140-6736(05)66544-0

4. Nahta R, Esteva FJ (2006) HER2 therapy: molecular mechanisms of trastuzumab resistance. Breast Cancer Res BCR 8:215. https://doi.org/10.1186/bcr1612

5. Abramson VG, Lehmann BD, Ballinger TJ, Pietenpol JA (2015) Subtyping of triple-negative breast cancer: implications for therapy. Cancer 121:8–16. https://doi.org/10.1002/cncr.28914

6. Mazerbourg S, Kuntz S, Grillier-Vuissoz I, et al (2016) Reprofiling of Troglitazone Towards More Active and Less Toxic Derivatives: A New Hope for Cancer Treatment? Curr Top Med Chem 16:2115–2124. https://doi.org/10.2174/1568026616666160216153036

7. Fröhlich E, Wahl R (2015) Chemotherapy and chemoprevention by thiazolidinediones. BioMed Res Int 2015:845340. https://doi.org/10.1155/2015/845340

8. Prost S, Relouzat F, Spentchian M, et al (2015) Erosion of the chronic myeloid leukaemia stem cell pool by PPARγ agonists. Nature 525:380–383. https://doi.org/10.1038/nature15248

9. Rousselot P, Prost S, Guilhot J, et al (2017) Pioglitazone together with imatinib in chronic myeloid leukemia: A proof of concept study. Cancer 123:1791–1799. https://doi.org/10.1002/cncr.30490

10. Smallridge RC, Copland JA, Brose MS, et al (2013) Efatutazone, an Oral PPAR-γ Agonist, in Combination With Paclitaxel in Anaplastic Thyroid Cancer: Results of a Multicenter Phase 1 Trial. J Clin Endocrinol Metab 98:2392–2400. https://doi.org/10.1210/jc.2013-1106

11. Ishay-Ronen D, Diepenbruck M, Kalathur RKR, et al (2019) Gain Fat-Lose Metastasis: Converting Invasive Breast Cancer Cells into Adipocytes Inhibits Cancer Metastasis. Cancer Cell 35:17-32.e6. https://doi.org/10.1016/j.ccell.2018.12.002

12. Chojkier M (2005) Troglitazone and liver injury: in search of answers. Hepatol Baltim Md 41:237–246. https://doi.org/10.1002/hep.20567

13. Salamone S, Colin C, Grillier-Vuissoz I, et al (2012) Synthesis of new troglitazone derivatives: anti-proliferative activity in breast cancer cell lines and preliminary toxicological study. Eur J Med Chem 51:206–215. https://doi.org/10.1016/j.ejmech.2012.02.044

14. Bordessa A, Colin-Cassin C, Grillier-Vuissoz I, et al (2014) Optimization of troglitazone derivatives as potent anti-proliferative agents: towards more active and less toxic compounds. Eur J Med Chem 83:129–140. https://doi.org/10.1016/j.ejmech.2014.06.015

15. Huang J-W, Shiau C-W, Yang J, et al (2006) Development of Small-Molecule Cyclin D1-Ablative Agents. J Med Chem 49:4684–4689. https://doi.org/10.1021/jm060057h

16. Shiau C-W, Yang C-C, Kulp SK, et al (2005) Thiazolidenediones mediate apoptosis in prostate cancer cells in part through inhibition of Bcl-xL/Bcl-2 functions independently of PPARgamma. Cancer Res 65:1561–1569. https://doi.org/10.1158/0008-5472.CAN-04-1677

17. Lecomte J, Flament S, Salamone S, et al (2008) Disruption of ERalpha signalling pathway by PPARgamma agonists: evidences of PPARgamma-independent events in two hormone-dependent breast cancer cell lines. Breast Cancer Res Treat 112:437–451. https://doi.org/10.1007/s10549-007-9886-z

18. Yang C-C, Ku C-Y, Wei S, et al (2006) Peroxisome proliferator-activated receptor gamma-independent repression of prostate-specific antigen expression by thiazolidinediones in prostate cancer cells. Mol Pharmacol 69:1564–1570. https://doi.org/10.1124/mol.105.018333

19. Colin C, Salamone S, Grillier-Vuissoz I, et al (2010) New troglitazone derivatives devoid of PPARγ agonist activity display an increased antiproliferative effect in both hormone-dependent and hormone-independent breast cancer cell lines. Breast Cancer Res Treat 124:101–110. https://doi.org/10.1007/s10549-009-0700-y

20. Colin-Cassin C, Yao X, Cerella C, et al (2015) PPARγ-inactive Δ2-troglitazone independently triggers ER stress and apoptosis in breast cancer cells. Mol Carcinog 54:393–404. https://doi.org/10.1002/mc.22109

21. Geoffroy M, Kleinclauss A, Grandemange S, et al (2017) Pro-apoptotic effect of Δ2-TGZ in "claudin-1-low" triple-negative breast cancer cells: involvement of claudin-1. Breast Cancer Res Treat 165:517–527. https://doi.org/10.1007/s10549-017-4378-2

22. Lehtimäki J, Hakala M, Lappalainen P (2017) Actin Filament Structures in Migrating Cells. Handb Exp Pharmacol 235:123–152. https://doi.org/10.1007/164_2016_28

23. Geoffroy M, Kleinclauss A, Kuntz S, Grillier-Vuissoz I (2020) Claudin 1 inhibits cell migration and increases intercellular adhesion in triple-negative breast cancer cell line. Mol Biol Rep. https://doi.org/10.1007/s11033-020-05835-3

24. Fife CM, McCarroll JA, Kavallaris M (2014) Movers and shakers: cell cytoskeleton in cancer metastasis. Br J Pharmacol 171:5507–5523. https://doi.org/10.1111/bph.12704

25. Rouleau A, Osta M, Lucchi G, et al (2012) Immuno-MALDI-MS in Human Plasma and On-Chip Biomarker Characterizations at the Femtomole Level. Sensors 12:15119–15132. https://doi.org/10.3390/s121115119

26. Colin C, Meyer M, Cerella C, et al (2018) Biotinylation enhances the anticancer effects of 15d-PGJ2 against breast cancer cells. Int J Oncol 52:1991–2000. https://doi.org/10.3892/ijo.2018.4338

27. Blanquicett C, Roman J, Hart CM (2008) Thiazolidinediones as anti-cancer agents. Cancer Ther 6:25–34

28. Motomura W, Nagamine M, Tanno S, et al (2004) Inhibition of cell invasion and morphological change by troglitazone in human pancreatic cancer cells. J Gastroenterol 39:461–468. https://doi.org/10.1007/s00535-003-1324-3

29. Wang P-S, Chou F-S, Porchia L, et al (2008) Troglitazone inhibits cell migration, adhesion, and spreading by modulating cytoskeletal rearrangement in human breast cancer cells. Mol Carcinog 47:905–915. https://doi.org/10.1002/mc.20429

30. Yang Y-C, Ho T-C, Chen S-L, et al (2007) Inhibition of cell motility by troglitazone in human ovarian carcinoma cell line. BMC Cancer 7:216. https://doi.org/10.1186/1471-2407-7-216

31. Folkman J, Moscona A (1978) Role of cell shape in growth control. Nature 273:345–349. https://doi.org/10.1038/273345a0

32. Sun X, Shi X, Liu M, et al (2011) Mdp3 is a novel microtubule-binding protein that regulates microtubule assembly and stability. Cell Cycle Georget Tex 10:3929–3937. https://doi.org/10.4161/cc.10.22.18106

33. Russu WA (2007) Thiazolidinedione anti-cancer activity: Is inhibition of microtubule assembly implicated? Med Hypotheses 68:343–346. https://doi.org/10.1016/j.mehy.2006.06.054

34. Kwon A, Lee GB, Park T, et al (2020) Potent Small-Molecule Inhibitors Targeting Acetylated Microtubules as Anticancer Agents Against Triple-Negative Breast Cancer. Biomedicines 8:. https://doi.org/10.3390/biomedicines8090338

35. Oba T, Ito K-I (2018) Combination of two anti-tubulin agents, eribulin and paclitaxel, enhances anti-tumor effects on triple-negative breast cancer through mesenchymal-epithelial transition. Oncotarget 9:22986–23002. https://doi.org/10.18632/oncotarget.25184

Figures

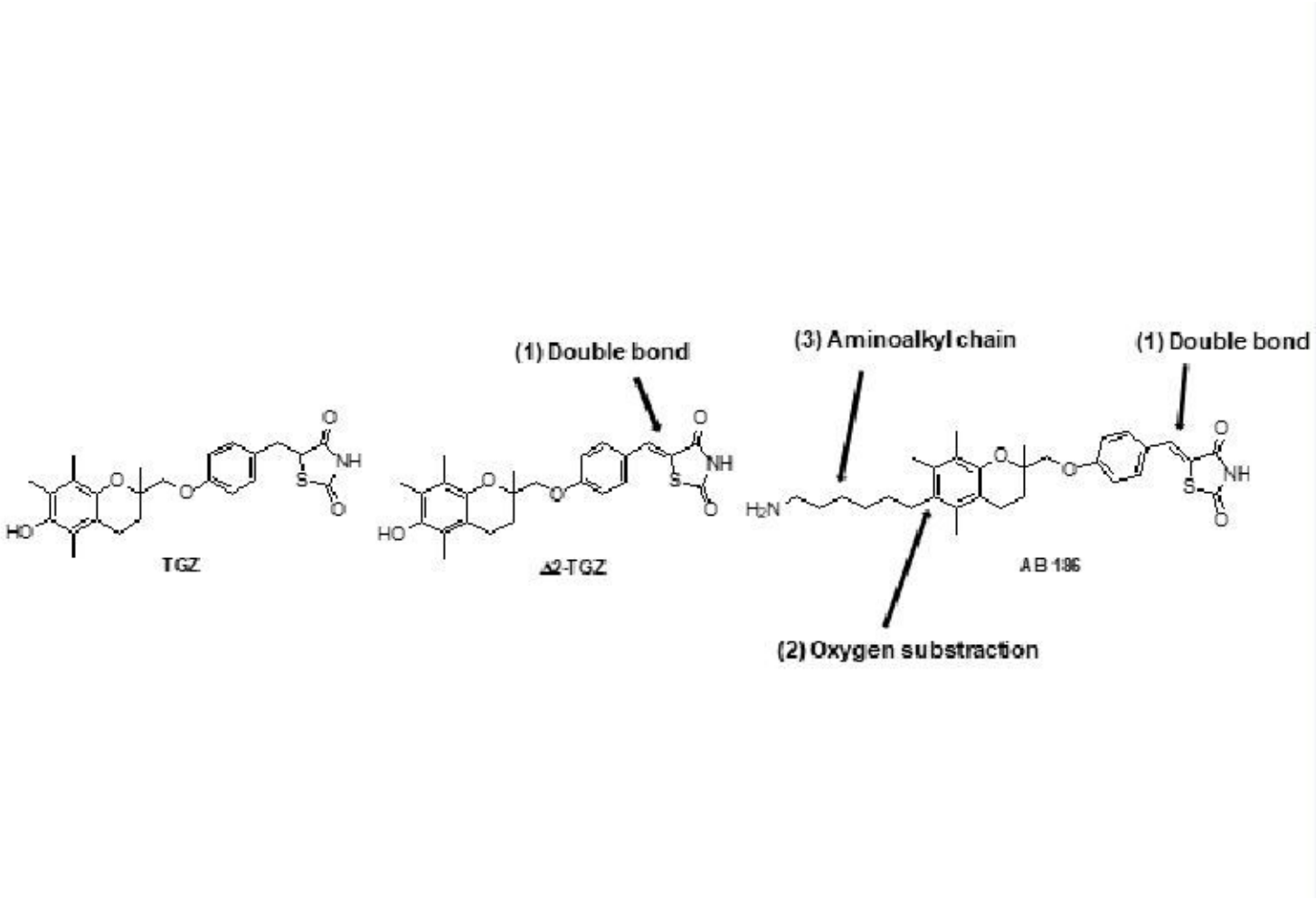

Figure 1

Structure of TGZ, Δ2-TGZ and AB186 compounds. Δ2-TGZ and AB186 are derived from the original TGZ and both of them possess a double bond (1) adjoining the terminal thiazolidine-2,4-dione ring. AB186 also presents a deoxygenation of the chromane heterocycle (2) and a hydrophobic moiety (3).

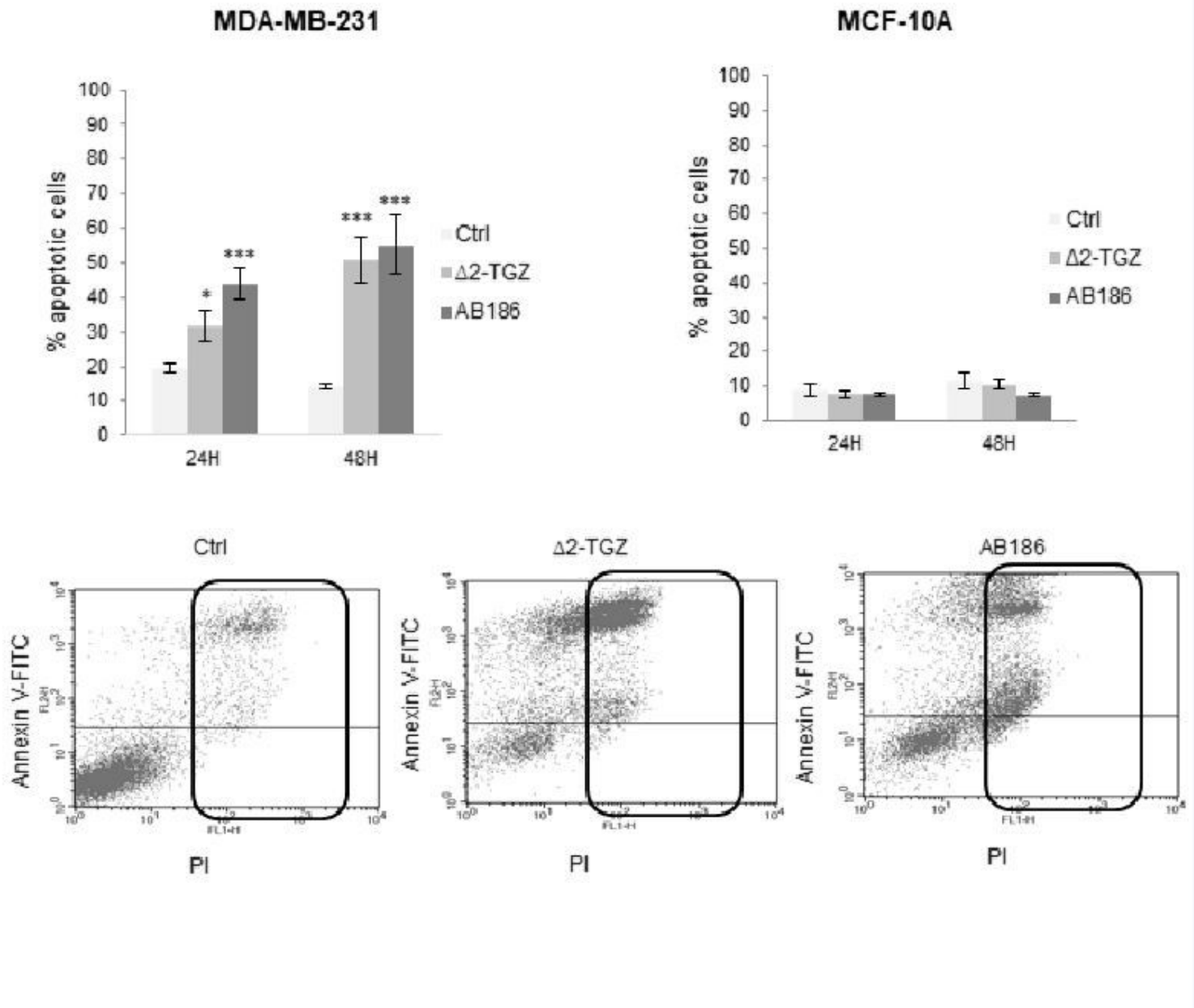

Figure 2

AB186 induces apoptosis in MDA-MB-231 TNBC cells. After treatment for 24 and 48 h with DMSO (Ctrl), 20 μM of Δ2-TGZ or 4 μM of AB186, MDA-MB-231 and MCF-10A cells were co-stained with FITC-Annexin V/PI and analyzed by FACS. The percentage of total apoptotic cells corresponds to Annexin V positive cells and Annexin V/PI positive cells (dot plot of MDA-MB-231 cells exposed to 48 h of treatment). The values represent the means ± SEM of 3 to 6 different experiments. ANOVA test with Bonferroni post-hoc was used to determine significance difference from control cells, were *p<0.05 and ***p<0.001.

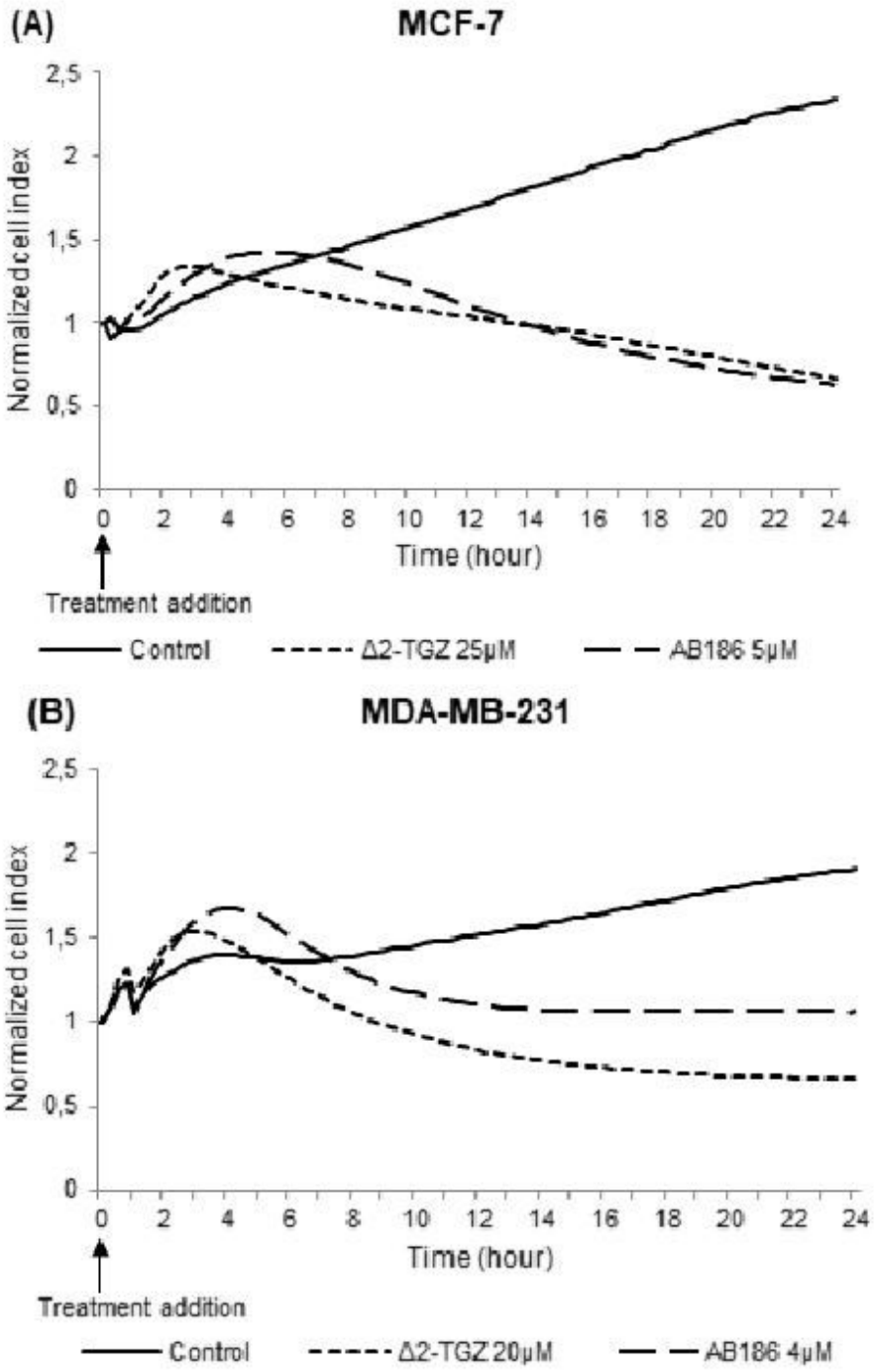

Figure 3

Kinetics of real-time impedance changes in response to TGZ derivatives in MDA-MB-231 and MCF-7 cells. (A) MCF-7 and (B) MDA-MB-231 cells were grown during 29 h and then were exposed (treatment addition) to Δ2-TGZ (25 µM and 20 µM respectively) or AB186 (5 µM and 4 µM respectively). Control cells were treated with DMSO. Cell index was monitored during 24 h after treatment addition. Reported data are the means of three independent experiments.

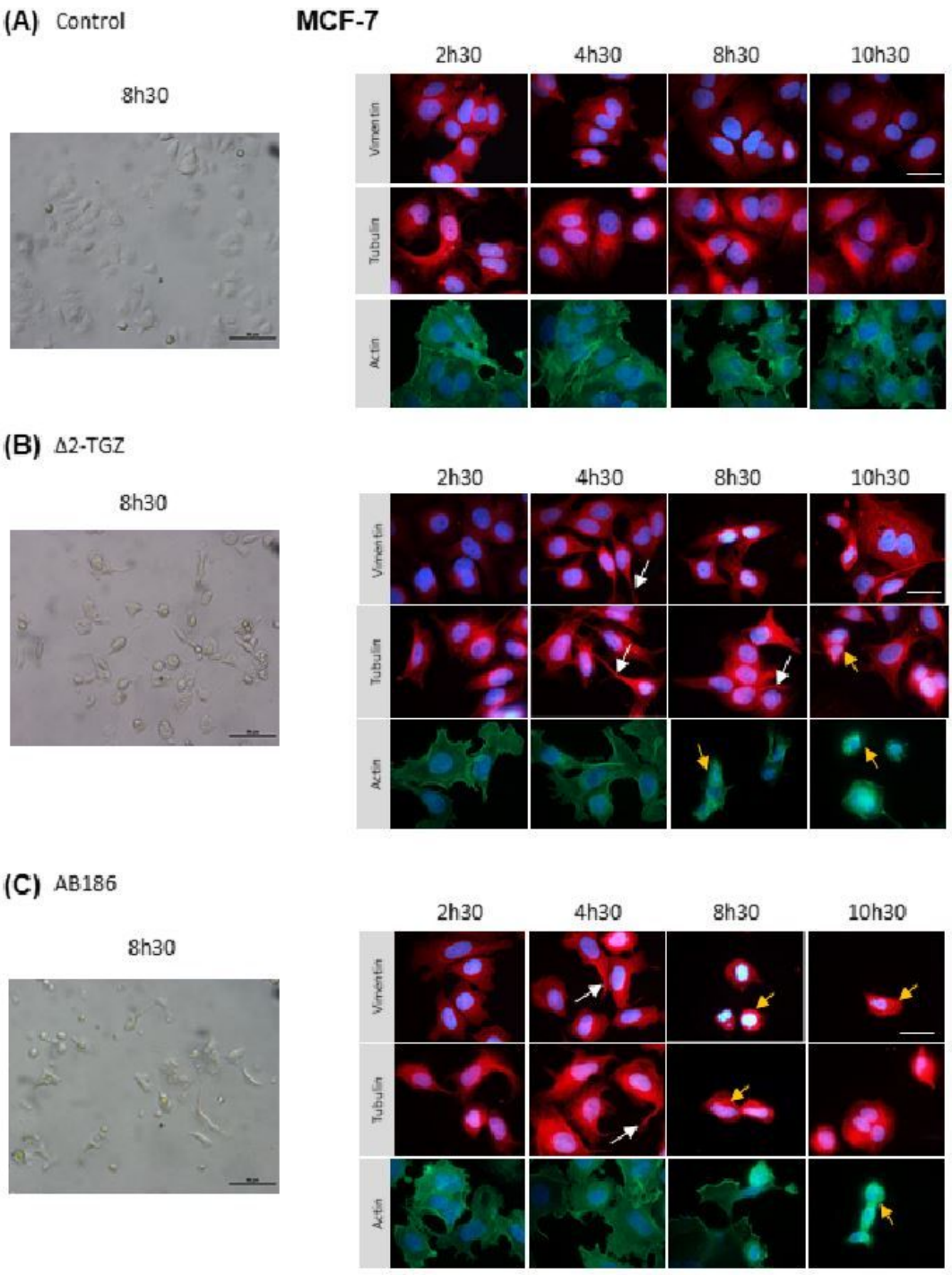

Figure 4

TGZ derivatives alter MCF-7 morphology. MCF-7 cells were treated with DMSO as control (A), 25 µM of Δ2-TGZ (B) or 5 µM of AB186 (C) during 2 h 30, 4 h 30, 8 h 30 and 10 h 30. Then, cells were subjected to immunofluorescence analysis and stained with antibodies against vimentin, α-tubulin and actin. Cell nuclei were labelled with Hoechst dye. Bright field pictures of control and treated cells are also shown after 8h30. Δ2-TGZ and AB186 led to disruption of cell-cell contact compared to untreated cells.

Elongated cells (white arrows) and some shrunken cells (yellow arrows) were observed. Bar represent 50 µm.

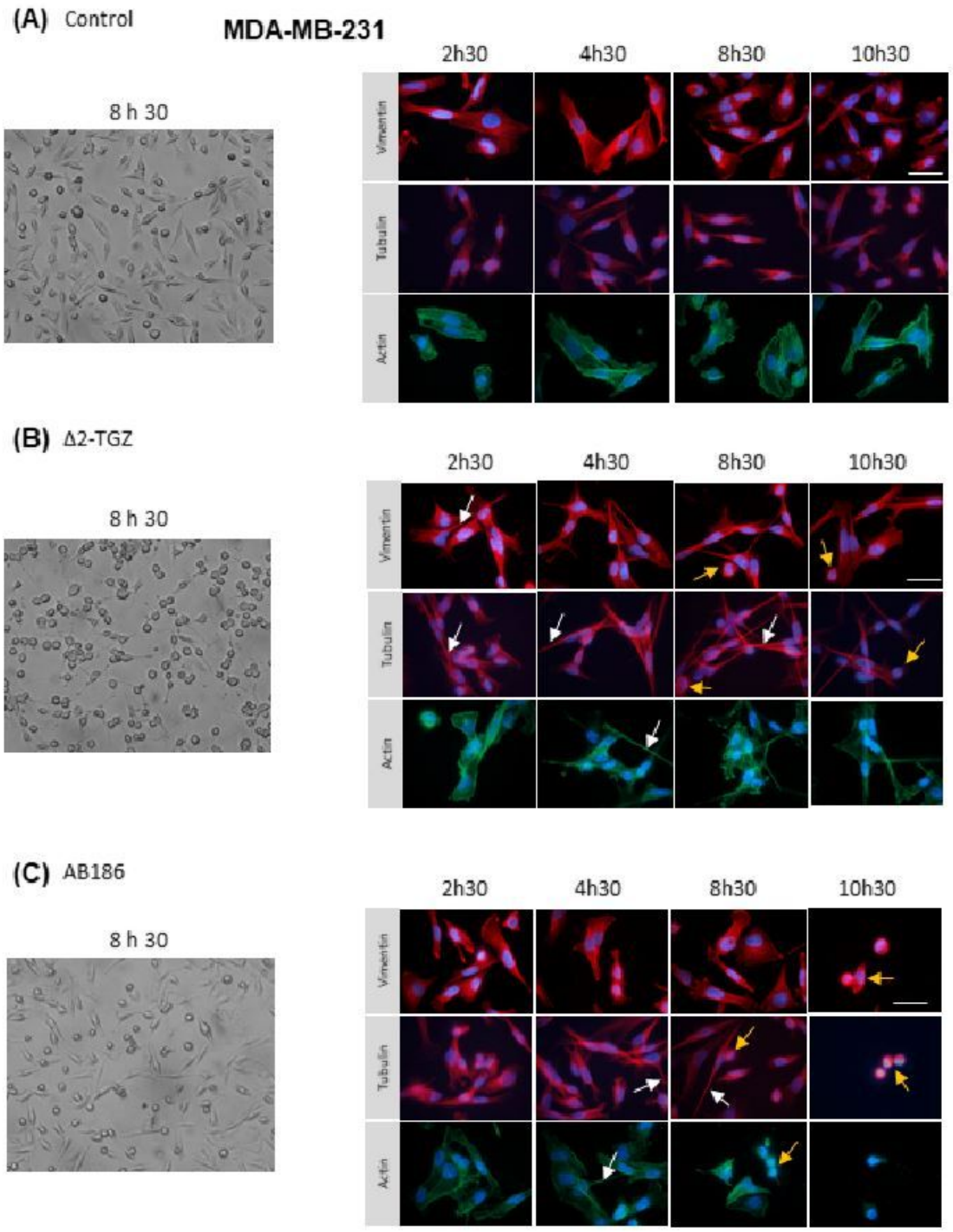

Figure 5

TGZ derivatives alter MDA-MB-231 morphology. MDA-MB-231 cells were treated with DMSO as control (A), 20 µM of Δ2-TGZ (B) or 4 µM of AB186 (C) during 2 h 30, 4 h 30, 8 h 30 and 10 h 30. Then, cells were subjected to immunofluorescence analysis and stained with antibodies raised against vimentin, α-tubulin

and actin. Cell nuclei were labelled with Hoechst dye. Bright field pictures of control and treated cells are also shown after 8h30. Elongated cells (white arrows) and some shrunken cells (yellow arrows) were observed. Bar represent 50 µm.

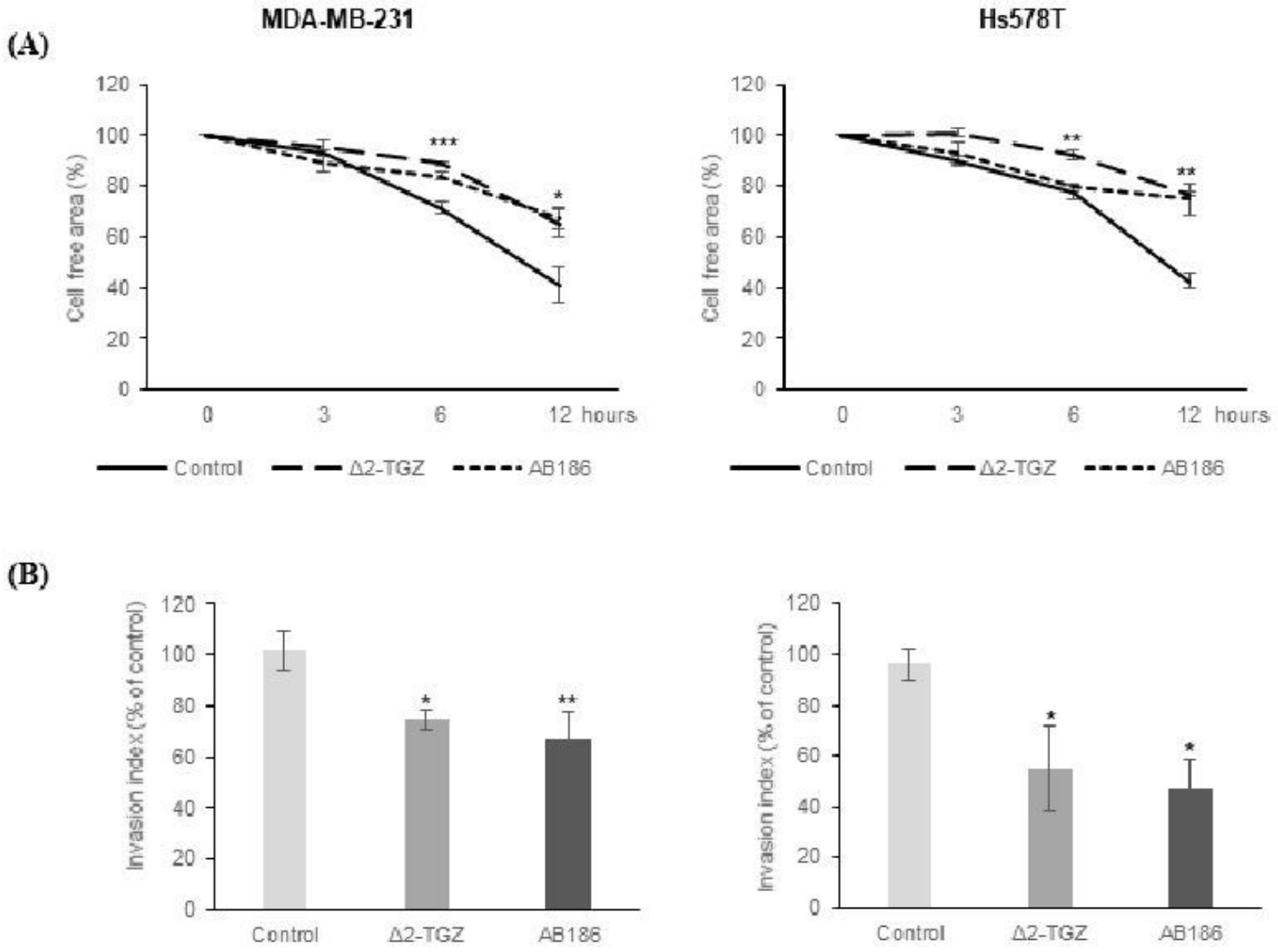

Figure 6

TGZ derivatives alter migration properties of MDA-MB-231 and Hs578T cells. MDA-MB-231 and Hs578T cells were exposed to DMSO as control, or 20 µM of Δ2-TGZ or 4 µM of AB186 and subjected to wound healing (A) or transwell migration (B) assays. (A) Cell free area was measured after 3 h, 6 h and 12 h of TGZ derivatives exposure. Each wound healing corresponds to the mean of three different areas. (B) Cells were seeded in the upper chamber of Transwell membranes and treated with Δ2-TGZ or AB186 for 9 h. Graphs represent the average of migrated cells on the lower chamber. Reported data are the means of three or six experiments. Analysis of variance (ANOVA) was used to determine significant difference of migration from control cells, where *p<0.05, **p<0.01 and ***p<0.001.

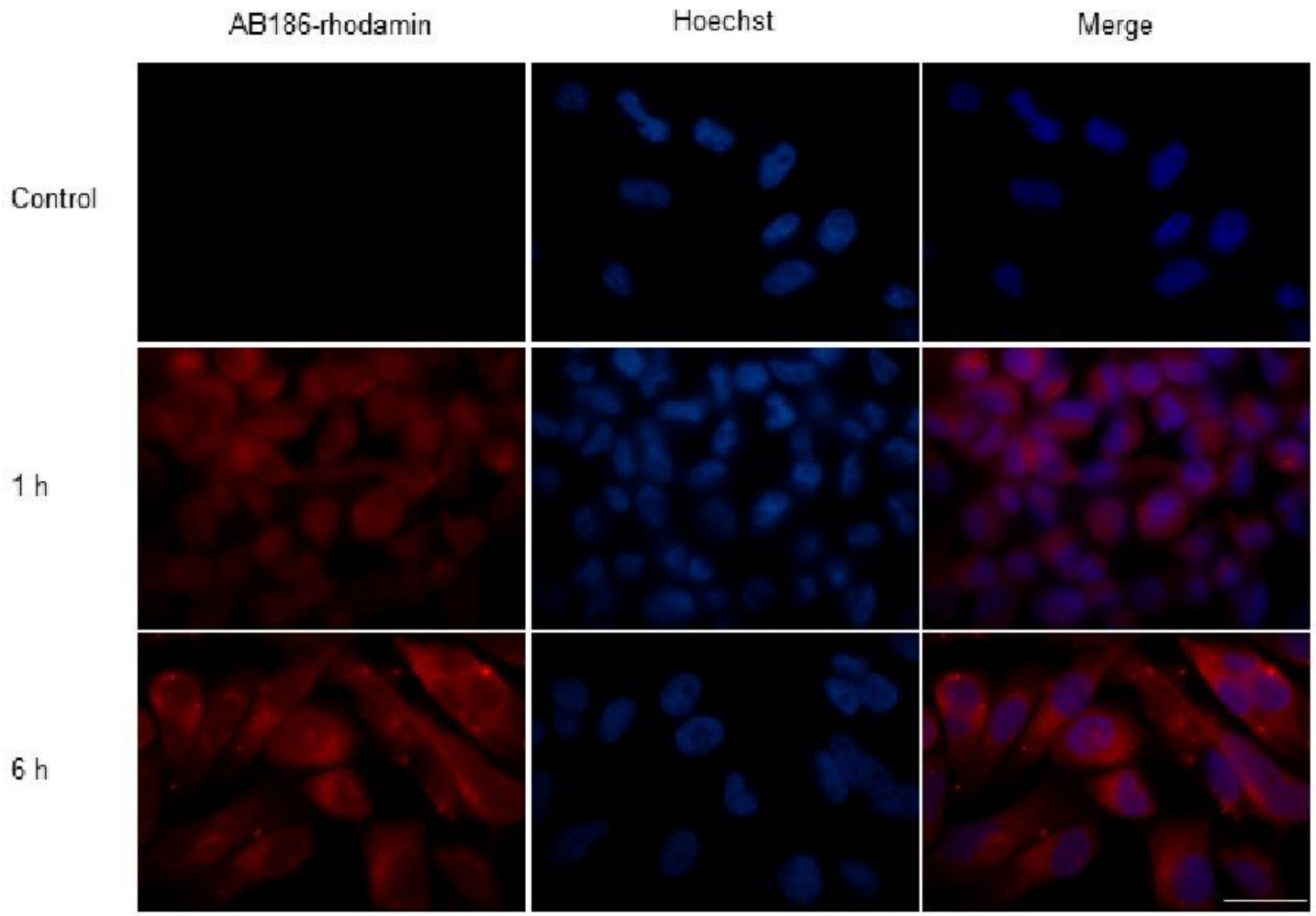

Figure 7

Rhodamin labelled AB186 localizes in the cytoplasm of MDA-MB-231 cells. MDA-MB-231 cells were exposed to 3 µM of Rhodamin labelled AB186 during 1 or 6 h. Control cells were exposed to the unlabeled compound. Cells were fixed with paraformaldehyde and cell nuclei were labelled with Hoechst dye. Bar represents 50 µm.

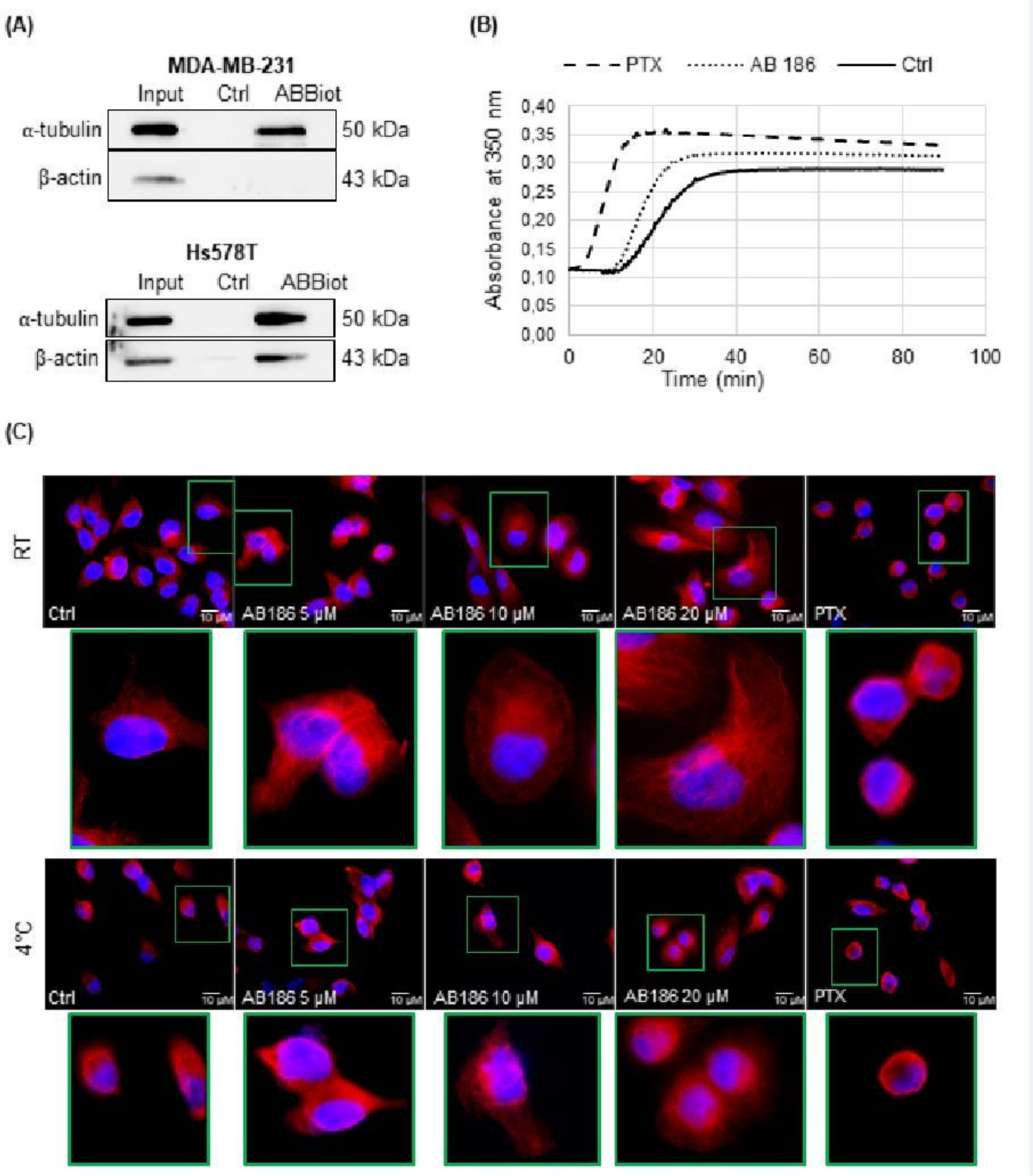

Figure 8

AB186 directly targets the microtubule cytoskeleton. (A) MDA-MB-231 and Hs578T cells lysate were incubated with the microbeads and biotinylated AB186 (ABBiot) for 40 minutes or in absence of AB186 (Ctrl). Precipitated proteins were then subjected to western blot analysis. Western blot analysis was performed using anti-α-tubulin and anti-β-actin antibodies. Input corresponds to the total lysate before pull-down assay. (B) In vitro tubulin polymerization assay was performed. Bovine tubulin was exposed to

DMSO (Ctrl), 5 µM of AB186 or 10 µM paclitaxel. The tubulin polymerization rate was monitored during 90 min at 37°C and measured by absorbance at 350 nm. (C) MDA-MB-231 cells were treated with DMSO (Ctrl), AB186 (5, 10 or 20 µM) or paclitaxel (PTX) (5 µM) during 15 min at room temperature (RT) or 4°C. Then, cells were subjected to immunofluorescence analysis after staining with antibodies raised against α-tubulin. Cell nuclei were labelled with Hoechst dye. Representative high-resolution image focusing on one single cell in each group present a 6X magnification. Bar represent 10 µm.

Supplementary Files

This is a list of supplementary files associated with this preprint. Click to download.

- Table1.jpg
- Table2.jpg
- Supplementarydata2.pdf